

Short communication

## Synthesis of NiO nanotubes for use as negative electrodes in lithium ion batteries

S.A. Needham\*, G.X. Wang, H.K. Liu

*Energy Storage Materials Group, Institute for Superconducting & Electronic Materials, University of Wollongong, Northfields Ave, Gwynneville NSW 2522, Australia*

Available online 30 May 2006

### Abstract

Nickel oxide (NiO) nanotubes have been produced for the first time via a template processing method. The synthesis involved a two step chemical reaction in which nickel hydroxide (Ni(OH)<sub>2</sub>) nanotubes were firstly formed within the walls of an anodic aluminium oxide (AAO) template. The template was then dissolved away using concentrated NaOH, and the freed nanotubes were converted to NiO by heat treatment in air at 350 °C. Individual nanotubes measured 60 μm in length with a 200 nm outer diameter and a wall thickness of 20–30 nm. The NiO nanotube powder was used in Li-ion cells for assessment of the lithium storage ability. Preliminary testing indicates that the cells demonstrate controlled and sustainable lithium diffusion after the formation of an SEI. Reversible capacities in the 300 mAh g<sup>-1</sup> range were typical.

© 2006 Elsevier B.V. All rights reserved.

*Keywords:* Li-ion batteries; Lithium storage; Nickel oxide; Template method; Nanotubes

### 1. Introduction

Li-ion batteries are now commonly utilized in popular electronic equipment, such as mobile telephones, laptop computers, and digital cameras. However, the next generation of portable appliances are being developed at an astounding rate. These new products will require more powerful and versatile energy storage systems. If Li-ion batteries are to be considered the battery of choice in the future, then significant improvements in the stored energy density and cyclability must occur. In addition, any advances in the performance of the battery must be achieved without sacrificing important safety aspects. For Li-ion batteries, the key to satisfying these objectives rests with the manufacture of electrode materials that have nanoscale dimensions (nanomaterials) [1].

It is well known that physical and chemical phenomena can be vastly different in a nanomaterial compared to those observed in its bulk state. This point is clearly illustrated in the transition metal oxide (MO) system (M=Fe, Co, Cu, Ni) by considering the applicability of these materials to Li-ion batteries. In this system, the reaction of the MO with lithium results in the formation of the reduced metal and lithia (Li<sub>2</sub>O). It had long

been reported that bulk Li<sub>2</sub>O was electrochemically inactive and therefore unable to be decomposed. However, by manufacturing nanostructured MO precursors, the resultant Li<sub>2</sub>O is also nanostructured and may be decomposed [2,3]. This finding has allowed the reaction of nanostructured MOs with lithium to be made completely reversible and meant that these materials have received significant attention as possible candidates for use in Li-ion batteries.

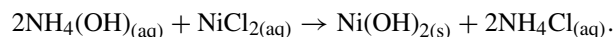
Early reports have shown that irregularly shaped MO nanoparticles can exhibit reversible capacities up to 700 mAh g<sup>-1</sup> [2]. This capacity is almost three times larger than that of the graphite based negative electrodes that are used in commercial rechargeable batteries. Of the wide range of nanostructures that are now feasible, the nanotube represents an ideal one-dimensional topology that can allow controlled Li<sup>+</sup> diffusion over many charge–discharge cycles [4]. This effect may be attributed to the high surface area and low diffusion distance for solid state Li-ion transport. Indeed, there have been recent reports on the synthesis of nanotubes made from V<sub>2</sub>O<sub>5</sub> [5,6], TiO<sub>2</sub> [7], and Co<sub>3</sub>O<sub>4</sub> [8] materials that demonstrate excellent electrochemical properties. However, progress on new transition MOs has been sparse, presumably due to the difficult nature of material synthesis. Nickel oxide is an important member of this group that shows potential as a chemical sensor and, in particular, as a negative electrode in Li-ion batteries.

\* Corresponding author. Tel.: +61 2 422 13733; fax: +61 2 422 15731.  
E-mail address: [scott\\_needham@uow.edu.au](mailto:scott_needham@uow.edu.au) (S.A. Needham).

In this paper, we report on the synthesis of uniform NiO nanotubes that are 60  $\mu\text{m}$  long with a 200 nm outer diameter and wall thickness of 20–30 nm. The synthesis involved first forming Ni(OH)<sub>2</sub> nanotubes within the walls of a commercially available anodic aluminium oxide (AAO) template. The AAO template was dissolved away by immersion in concentrated NaOH solution. The released nickel hydroxide nanotube bundles were converted to NiO by heat treatment without any alteration of the nanotubular structure. Physical characterisation of the NiO nanotubes is presented by SEM and TEM techniques along with a preliminary assessment of the electrochemical performance for Li-ion battery applications.

## 2. Experimental

NiO nanotubes 60  $\mu\text{m}$  long with an outer wall diameter of 200 nm and wall thickness of 20–30 nm were synthesized by using an AAO template. The first stage in this process was to synthesise Ni(OH)<sub>2</sub> nanotubes inside a commercially available anodic aluminium oxide template (Whatman, UK). The template was soaked in a 0.5 M NiCl<sub>2</sub> solution to impregnate the walls of the template with nickel ions. A 2 M NH<sub>4</sub>OH solution was then dripped slowly onto the template using a laboratory grade micropipette. Gravitational forces gradually coerced the ammonia solution through the pores which reacted with nickel ions to precipitate Ni(OH)<sub>2</sub> tubes. The overall chemistry is represented by the following double displacement reaction:



Excess hydroxide precipitate was cleaned from the top and bottom surfaces of the template using a laboratory wipe. Insufficient cleaning of the template resulted in the formation of a thick Ni(OH)<sub>2</sub> layer. Nanotube bundles were released by dissolving the template in a 2 M NaOH solution for 2 h. The product was then centrifuged several times in deionised H<sub>2</sub>O and then finally acetone. The Ni(OH)<sub>2</sub> nanotubes were converted to bunsenite NiO nanotubes by heat treatment in air at 350 °C for 1 h.

The composition and structure of the precursor and converted powders was determined using a Philips PW1730 X-ray diffractometer with monochromatised Cu K $\alpha$  radiation ( $\lambda = 1.5418 \text{ \AA}$ ). The morphology of the powders was observed by a JEOL JSM-6460A scanning electron microscope (SEM) and JEOL 2010 transmission electron microscope (TEM).

Working anodes were prepared by combining 82 wt.% NiO nanotube powder, 8 wt.% carbon black (Lexel, 99%) as a conducting agent, and 12 wt.% polyvinylidene fluoride (Aldrich, 99%) as a binder. After being blended in several drops of *N*-methylpyrrolidinone, the mixed slurry was spread uniformly on 1 cm<sup>2</sup>  $\times$  0.1 mm thick copper foil (99.99%) substrate. The electrodes were dried in a vacuum oven for 24 h at 70 °C then cold pressed at 200 kg cm<sup>-2</sup> in a uniaxial hydraulic press. Electrodes contained no more than 1 mg of active material (NiO nanotube powder). Standard CR 2032 type coin cells were assembled in a high purity argon filled glove box (H<sub>2</sub>O < 5 ppm, O<sub>2</sub> < 30 ppm) using the NiO nanotube powder as the working electrode and battery grade lithium foil as the counter and reference electrodes. Celgard 2400 was used as the separator membrane and 1 M

LiClO<sub>4</sub> and ethylene carbonate (EC)/diethyl carbonate (DEC) at 1:1 (v/v) was used as the electrolyte. Cyclic voltammograms (CVs) were measured using a CH Instruments electrochemical workstation (CHI 660A) at a scan rate of 0.2 mV s<sup>-1</sup> between 0.01 and 3.0 V versus Li/Li<sup>+</sup>. Charge–discharge cycles of the half-cells were measured between 0.025 and 3.0 V versus Li/Li<sup>+</sup> at an average constant current density of 0.025 A g<sup>-1</sup> using a Neware battery cyler in galvanostatic mode. Current density and specific capacity was calculated based on the mass of active material in the electrode. All electrochemical testing was carried out at ambient temperature (23  $\pm$  2 °C).

## 3. Results and discussion

### 3.1. Materials characterization

The purity and crystallinity of the Ni(OH)<sub>2</sub> precursor nanotubes and NiO nanotubes were examined by XRD as shown in Fig. 1. The hydroxide nanotubes in Fig. 1(a) correspond closely with the  $\alpha$ -Ni(OH)<sub>2</sub> phase (JCPDS-ICDD card 38-0715). The diffraction pattern indicates two primary peaks at 11.3 and 23.5° ((003) and (006) reflections, respectively) and two of the minor peaks at 35 and 63° ((012) and (110) reflections, respectively). In addition, the orientation of layers in the  $\alpha$ -phase is completely random, although the interlayer separation remains constant. It is this turbostratic character that accounts for the poor crystallinity of the tubes as assessed by significant peak broadening.

The diffraction pattern of the NiO nanotubes in Fig. 1(b) corresponds well with standard crystallographic data (JCPDS-ICDD card 01-1237, Bunsenite mineral). The structure is a cubic unit cell with three main diffraction peaks at 37.4, 43.5, and 62.6° ((111), (200), and (220) reflections, respectively). Despite the full conversion to the ordered cubic unit cell, the overall morphology of the nanotubes remained nanocrystalline. This phenomenon is thought to be characteristic of the fine tubular structure.

Fig. 2 shows representative SEM images of NiO nanotubes. Fig. 2(a) demonstrates the process of template dissolution and concomitant appearance of the nanotubes. It can be seen that nanotubes of  $\sim$ 10  $\mu\text{m}$  in length are protruding from the

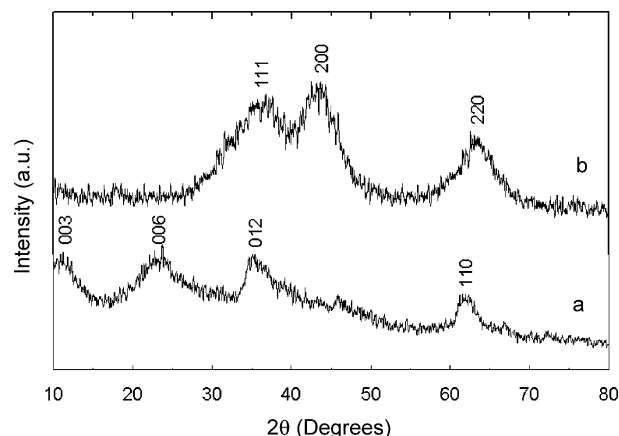


Fig. 1. X-ray diffraction patterns of (a) Ni(OH)<sub>2</sub> nanotubes and (b) NiO nanotubes.

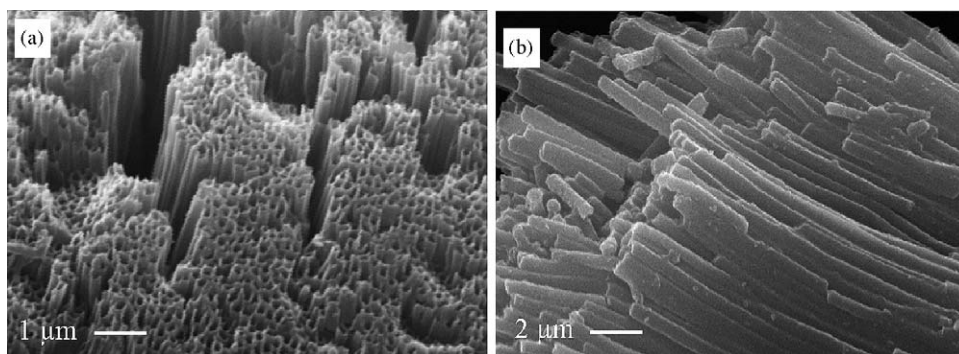


Fig. 2. SEM images of NiO nanotube bundles after conversion from Ni(OH)<sub>2</sub> by heat treatment at 350 °C in air (a), and a higher magnification view of NiO nanotube strands (b).

partially dissolved AAO template below. Complete dissolution of the AAO template releases bundles of tubes that are 60 μm in length (the thickness of the AAO template). Fig. 2(b) is an SEM image of the tubes from the side, which demonstrates their parallel arrangement and smooth surface alignment. It is feasible that the nanotubes have aggregated into bundles due to their high surface energy or van der Waals forces as seen in CuO nanorods [9]. Vast bundles of tubes ranging from a micron to several tens of microns wide were typical. The bundles were able to be broken down into individual nanotubes through ultrasonication. Additional qualitative analysis was obtained by TEM as shown in Fig. 3. The tubular shape of the material was further confirmed by observing that the central parts of the mesostructure are bright in comparison to the edges. Tube walls are well developed and are composed of an array of nanoparticles that resemble the scales on a fish.

### 3.2. Electrochemical characteristics of NiO nanotubes

Cyclic voltammetry measurements were performed to examine the electrochemical properties of the NiO nanotube powders. Fig. 4 presents the first two complete cycles performed at a sweep rate of 0.2 mV s<sup>-1</sup> from 0.01 to 3.0 V. The first discharge for the

NiO nanotube electrode shows an irreversible reduction peak with a maximum at 0.9 V. This is most likely caused by the electrochemical formation of a SEI layer and the decomposition of NiO to metallic nickel [10,11]. On the first charge, there is a broad anodic shelf that stretches from 1.5 to 2.3 V. This corresponds to the reverse process where Ni is reoxidised to NiO and Li<sub>2</sub>O decomposes. In the subsequent cycle, the reduction peak shifts to 0.7 V, while the oxidation peak is more prominent at 1.5 V.

Fig. 5 shows the cycling behaviour of NiO nanotube electrodes at an average current density of 0.025 mAh g<sup>-1</sup>. The capacity of the NiO nanotube electrodes decreases sharply in the first few cycles. This represents a significant and prolonged irreversible capacity loss that may be explained by the surface based nature of the reaction process. The electrochemical reactivity of the NiO begins high due to the use of high surface area nanotubes. Once initial cycling commences, the NiO is reduced to metallic nickel with even finer dimensions. This further enhances the electrochemical reactivity as grains divide. Electrochemically divided transition metals (Ni, Co, Fe, etc.) are known to have excellent catalytic activity. The formation of these may have enhanced electrolyte decomposition and led to the extended formation of a SEI. Work on CuO has shown this

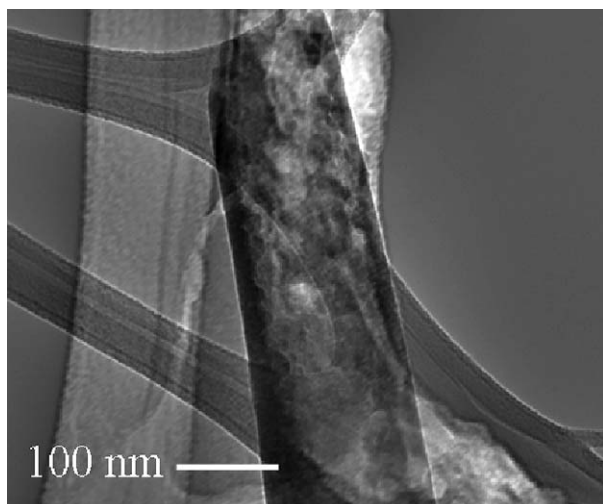


Fig. 3. TEM bright field image of an individual NiO nanotube.

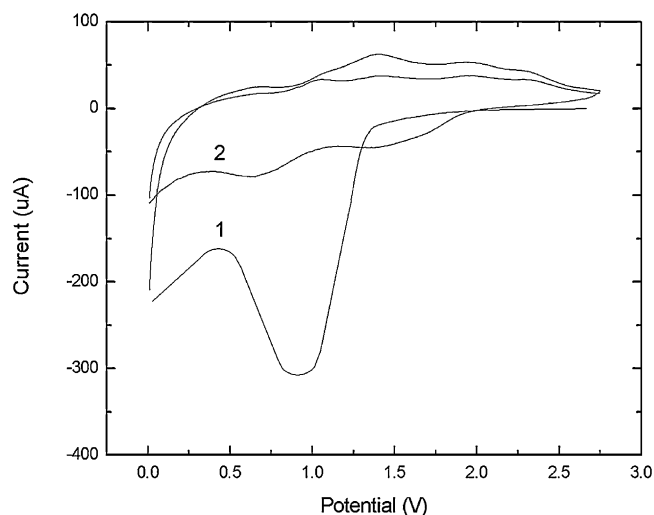


Fig. 4. CV curve of NiO nanotube electrode obtained at a sweep rate of 0.2 mV s<sup>-1</sup>.

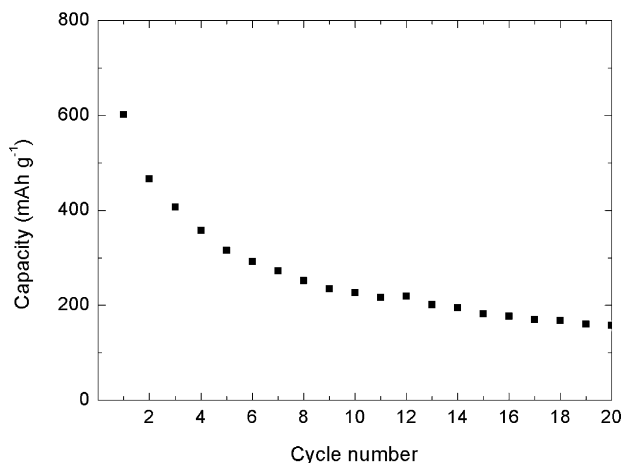


Fig. 5. Discharge capacity of a NiO nanotube electrode obtained at a constant current density of  $0.025 \text{ mAh g}^{-1}$ .

layer to be a thick translucent film that surrounded the CuO particles [9]. It is possible that the formation of the SEI in the present study is similar to that observed for CuO where the thickness of this layer gradually increases with cycling up to a limiting thickness. During the formation of this film, charge transfer would be increasingly hindered. This phenomenon may explain the observed high irreversible capacity loss up to about 10 cycles. After 10 cycles, the discharge capacity is stable. In this way, the SEI in the NiO nanotube electrode would be completely formed after 10 cycles, therefore allowing a more controlled and sustainable Li diffusion after this time.

#### 4. Conclusions

Nickel oxide (NiO) nanotubes have been successfully produced by a template synthesis technique. The tubes are  $60 \mu\text{m}$  long,  $200 \text{ nm}$  in outer diameter, and have a wall thickness of

$20\text{--}30 \text{ nm}$ . Preliminary electrochemical testing of NiO nanotube electrodes indicates a large irreversible capacity loss which limits their application in rechargeable lithium batteries. Our results also demonstrate that template synthesis techniques can be an effective method for producing experimental quantities of high aspect ratio NiO nanotubes. This technique may be applied to produce nanotubes of other transition MOs in order to assess their suitability for use in rechargeable lithium batteries.

#### Acknowledgement

The authors would like to acknowledge financial support provided by the Australian Research Council (Linkage Project LP0453766).

#### References

- [1] G.R. Patzke, F. Krumeich, R. Nesper, *Angew. Chem. Int. Ed.* 41 (2002) 2446.
- [2] P. Poizot, S. Laruelle, S. Grugeon, L. Dupont, J.-M. Tarascon, *Nature* 407 (2000) 496.
- [3] M.N. Obrovac, R.A. Dunlap, R.J. Sanderson, J.R. Dahn, *J. Electrochem. Soc.* 148 (6) (2001) A576.
- [4] W.Y. Li, L.-N. Xu, J. Chen, *Adv. Funct. Mat.* 15 (5) (2005) 851.
- [5] A. Augustsson, T. Schmitt, L.-C. Duda, J. Nordgren, S. Nordlinder, K. Edstrom, T. Gustafsson, J.-H. Guo, *J. Appl. Phys.* 94 (8) (2003) 5083.
- [6] L. Mai, W. Chen, Q. Xu, Q. Zhu, C. Han, J. Peng, *Solid State Comm.* 126 (2003) 541.
- [7] S.M. Liu, L.M. Gan, L.H. Liu, W.D. Zhang, H.C. Zeng, *Chem. Mater.* 14 (2002) 1391.
- [8] Y.-N. Nuli, S.-L. Zhao, Q.-Z. Qin, *J. Power Sources* 114 (2003) 113.
- [9] X.P. Gao, J.L. Bao, G.L. Pan, H.Y. Zhu, P.X. Huang, F. Wu, D.Y. Song, *J. Phys. Chem. B* 108 (2004) 5547.
- [10] S. Grugeon, S. Laruelle, R. Herrera-Urbina, L. Dupont, P. Poizot, J.-M. Tarascon, *J. Electrochem. Soc.* 148 (4) (2001) A285.
- [11] P. Poizot, S. Laruelle, S. Grugeon, L. Dupont, J.-M. Tarascon, *J. Power Sources* 97–98 (2001) 235.